



Room-temperature ferromagnetism in the mixtures of the TiO_2 and Co_3O_4 powders

A. Serrano,¹ E. Fernandez Pinel,² A. Quesada,^{2,3} I. Lorite,⁴ M. Plaza,¹ L. Pérez,¹ F. Jiménez-Villacorta,^{3,5} J. de la Venta,¹ M. S. Martín-González,⁶ J. L. Costa-Krämer,⁶ J. F. Fernandez,⁴ J. Llopis,¹ and M. A. García^{1,4,*}

¹*Dpto. Física de Materiales, Universidad Complutense de Madrid, 28040 Madrid, Spain*

²*Instituto de Magnetismo Aplicado, UCM, Las Rozas, 28230 Madrid, Spain*

³*Instituto de Ciencia de Materiales de Madrid, CSIC, 28049 Madrid, Spain*

⁴*Instituto de Cerámica y Vidrio, CSIC, 28049 Madrid, Spain*

⁵*SpLine, Spanish CRG Beamline at the ESRF, 38043 Grenoble, France*

⁶*Instituto de Microelectrónica de Madrid, CSIC, Tres Cantos, 28760 Madrid, Spain*

(Received 11 December 2008; published 3 April 2009)

We report here the observation of ferromagnetism (FM) at 300 K in mixtures of TiO_2 and Co_3O_4 powders despite the antiferromagnetic and diamagnetic characters of both oxides, respectively. The ferromagnetic behavior is found in the early stages of reaction and only for TiO_2 in anatase structure; no FM is found for identical samples prepared with rutile- TiO_2 . Optical spectroscopy and x-ray absorption spectra confirm a surface reduction of octahedral $\text{Co}^{+3} \rightarrow \text{Co}^{+2}$ in the mixtures which is in the origin of the observed magnetism.

DOI: [10.1103/PhysRevB.79.144405](https://doi.org/10.1103/PhysRevB.79.144405)

PACS number(s): 75.70.-i, 75.30.Et, 75.50.Gg, 78.40.-q

I. INTRODUCTION

The appearance and control of magnetism in traditionally nonmagnetic oxides are nowadays some of the most active and pursued goals of material physics.¹ In the last years, research has been focused mainly on oxides doped with magnetic ions (the so-called diluted magnetic semiconductors). Recent results^{2–5} indicate that the appearance of magnetism in these oxides (mainly ZnO and TiO_2) is related to the presence of defects and surface/interface effects^{6,7} but the origin of most of the experimental results is still unclear.⁸ Actually, results are hardly reproducible and findings from different groups are commonly contradictory. Understanding this lack of reproducibility is probably one of the main challenges to determine the origin of this magnetism.

A common feature of all the experimental observations of this magnetism is that signals are very weak, suggesting that only few atoms are involved in the magnetic response. Thus, it has been proposed that the emerging magnetism in oxides corresponds to surface/interface magnetism.^{9–11}

It is really tough understanding the origin of this magnetism based only on magnetic measurements since signals are very weak and effects from the rest of the material as impurities could mask the signals coming from interfaces. In this framework, correlating the magnetic properties with other measurements, sensitive to the electronic structure, can help to clarify this magnetism. This is the case of optical measurements as the energy of photons involved in the processes allows discrimination between different processes produced in different atoms. Furthermore, optical properties are particularly sensitive to surfaces as the broken symmetry of the surface induces new electronic levels (surface states) so that they can be especially useful for the investigation of surface effects.

In this work we study the magnetic properties of TiO_2 and Co_3O_4 . Both oxides are mixed in powder form and thermal treated to promote their interaction. Optical and x-ray absorption measurements are used to identify the origin of the observed room-temperature magnetism. The difficulties to

reproduce experiments in this kind of materials are also addressed.

II. EXPERIMENTAL

Samples were prepared by mixing powders of TiO_2 in anatase (*A*- TiO_2) and rutile structure (*R*- TiO_2) with 1 and 5 wt % Co_3O_4 . Analytical grade powders were selected with average particles size in the submicronic range, typically 0.3–0.4 μm (see Fig. 1). Pure powders were tested in order to ensure that no ferromagnetic contributions were present. TiO_2 powder showed diamagnetic behavior and Co_3O_4 paramagnetic one. When subtracting the paramagnetic behavior, some Co_3O_4 samples exhibited a weak ferromagneticlike contribution with magnetization below $5 \cdot 10^{-4}$ emu/g that disappeared after annealing at 400 °C.¹¹ This residual magnetization due to trace impurities was taken into account and adequately subtracted from the magnetic measurement of mixtures. Any powder with higher ferromagneticlike behavior was considered as contaminated and completely discarded. Initially, the powders were mixed and milled in an attrition mill with zirconia balls for 15 min, and subsequently they were thermally treated in air for 12 h at different temperatures between 500 and 900 °C. Selected raw materials were also processed following the same procedure to verify experimental conditions. Three different sets of samples were independently prepared at different laboratories (corresponding to authors' affiliations 1, 2, and 3). Processing was

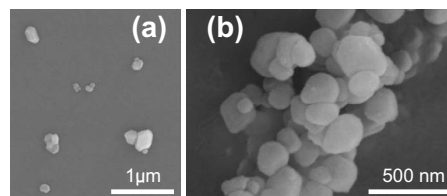


FIG. 1. Scanning electron microscopy (SEM) images from (a) initial Co_3O_4 powder. (b) 99%A- TiO_2 -1% Co_3O_4 sample milled.

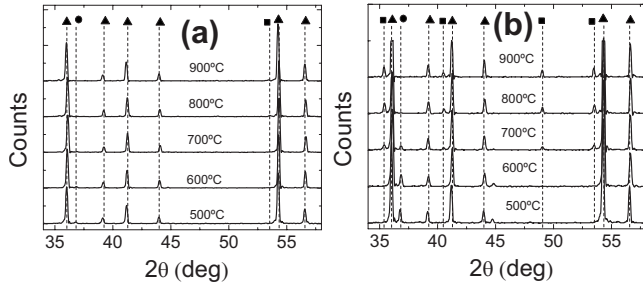


FIG. 2. XRD patterns from *R*-TiO₂ with (a) 1 mol % of Co₃O₄ and (a) 5 mol % of Co₃O₄. Symbols stand for (▲) TiO₂ rutile, (●) Co₃O₄, and (■) CoTiO₃.

managed without using any kind of metallic tools to prevent contamination

The structural analysis of the samples was carried out with a Siemens D5000 x-ray diffractometer (XRD) using a monochromatic Cu K line and operating at 40 kV and 40 mA. Magnetic characterization was performed in three different vibrating sample magnetometers (VSMs): VSM LDJ instruments, Quantum Design physical properties measurement system (PPMS)-VSM, and VSM Lakeshore 7304. For the magnetic measurements, all possible sources of experimental errors described in Ref. 12 were taken into account. Optical absorption was measured with a Shimadzu 3101 spectrophotometer attached with an integrating sphere. X-ray absorption spectroscopy (XAS) was performed at beamline BM25 (SpLine) in the European Synchrotron Radiation Facility at Grenoble.

III. RESULTS AND DISCUSSION

Figure 2 presents XRD measurements for the samples prepared using *R*-TiO₂. Up to annealing temperatures of 600 °C only the initial *R*-TiO₂ and Co₃O₄ phases are observed in the XRD patterns. After annealing at 700 °C, some peaks from CoTiO₃ appear for the samples with 5% Co₃O₄, coexisting with the initial phases. These data confirm that the reaction between both phases has started at this temperature. The peaks are scarcely identified for the samples with 1% Co₃O₄. This is quite reasonable since the amount of CoTiO₃ that can be formed is limited mainly by the concentration of Co₃O₄ in the sample. Thus, the differences between both samples seem more related to the detection limit of the experimental setup than to structural differences. As the temperature increases over 700 °C, the peaks from CoTiO₃ also do, while the Co₃O₄ ones decrease, disappearing at 800 °C. At this temperature, all the Co₃O₄ in the sample have reacted with the TiO₂ forming CoTiO₃. Due to the small fraction of Co₃O₄, there is an excess of TiO₂ that remains unaltered in the sample at all annealing temperatures, as evidenced in the XRD patterns.

Summarizing, the annealing process induces the interaction between both phases, consisting in the reaction of the Co₃O₄ with a small amount of *R*-TiO₂ to form CoTiO₃. The reaction starts below 700 °C and is completed over 800°, when all the Co₃O₄ have reacted to form the spinel phase that coexists with the excess of *R*-TiO₂.

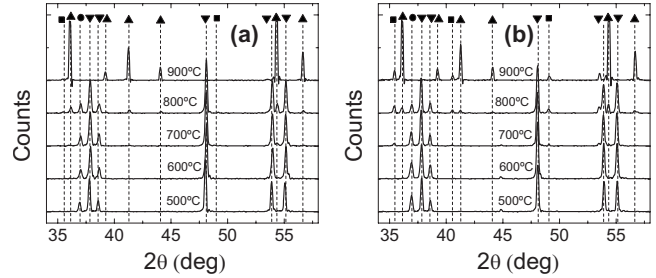


FIG. 3. XRD patterns from *A*-TiO₂ with (a) 1 mol % of Co₃O₄ and (a) 5 mol % of Co₃O₄. Symbols stand for (▼) TiO₂ anatase, (▲) TiO₂ rutile, (●) Co₃O₄, and (■) CoTiO₃.

The XRD patterns from the samples prepared with *A*-TiO₂ are more complicated (Fig. 3). As in the case of *R*-TiO₂, up to 600 °C only the initial phases are observed in the XRD diffractograms. After annealing at 700 °C the presence of scarce peaks, ascribed to CoTiO₃, coexisting with the initial phases, indicates a partial reaction. Simultaneously, peaks from *R*-TiO₂ are shown, confirming that the transformation of *A*-TiO₂ → *R*-TiO₂ has started at this temperature. The presence of CoTiO₃ increases with the temperature of the thermal treatment, while the transformation of *A*-TiO₂ → *R*-TiO₂ is completed at 900 °C. At this temperature, only *R*-TiO₂ and CoTiO₃ are present in the sample (as for the samples prepared with *R*-TiO₂).

Therefore, for these samples, the annealing produces two simultaneous processes: the reaction of TiO₂ with Co₃O₄ (similar to that produced in samples with *R*-TiO₂) and the transformation *A*-TiO₂ → *R*-TiO₂.

Magnetic characterization of the samples is presented in Fig. 4. The overall behavior is paramagnetic with susceptibility decreasing up to annealing temperature of 500 °C and increasing for higher temperatures. According to XRD diffractograms, the increase in magnetic susceptibility is due to

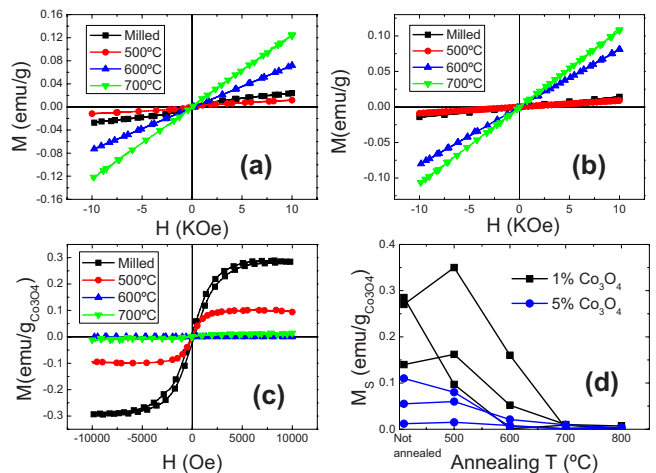


FIG. 4. (Color online) Magnetization curves for 99%TiO₂-1%Co₃O₄ samples annealed at different temperatures for (a) *A*-TiO₂ and (b) *R*-TiO₂. (c) Curves for the samples with TiO₂ in anatase structure after subtraction of a paramagnetic (linear) component. (d) Saturation magnetization of the ferromagnetic component for the samples prepared with *A*-TiO₂ with 1 and 5 wt % of Co₃O₄.

the reaction of the Co_3O_4 with the TiO_2 to form CoTiO_3 that has larger magnetic susceptibility than Co_3O_4 .^{13,14} Differences in the value of magnetic susceptibility for rutile and anatase samples can be explained in terms of the different kinetic of the reaction with Co_3O_4 . Rutile exhibits a more closed structure than anatase,¹⁵ so the reaction with Co_3O_4 is slower than for anatase, which exhibits a more opened structure and is therefore more reactive. Hence, for a fixed temperature, the degree of transformation is smaller for rutile, and the magnetic susceptibility decreases accordingly (as the transformed CoTiO_3 exhibits larger susceptibility).

Despite the diamagnetic character of TiO_2 and the antiferromagnetic behavior of Co_3O_4 and CoTiO_3 (with Néel temperatures of 42 and 37 K, respectively), we found a ferromagnetic contribution at room temperature for the samples with Co_3O_4 and A- TiO_2 milled and after annealing at low 500 and 600 °C [Fig. 4(c)]; this contribution is not observed in the R - TiO_2 samples in all range of temperatures.

The experiment was repeated three different times at different laboratories, using oxides from different suppliers with similar specifications and different experimental setups. While the quantitative results are different [see Fig. 4(d)], in all three cases we found the same effect: ferromagnetism at room temperature is only observed when using A- TiO_2 structure and after annealing at low temperature (below 700 °C). Quantitative differences appear in the maximum value of M_S , which ranges from $3.6 \cdot 10^{-1}$ to $1 \cdot 10^{-1}$ emu/g Co_3O_4 . The highest M_S in the presented data appears after milling, while for the other two sets it is found after 500 °C of annealing [Fig. 4(d)]. For the samples with 5% Co_3O_4 , the effect also exists, although the value of M_S is fairly smaller than for those samples with 1% Co_3O_4 . The paramagnetic component, on the other hand, is found to be basically the same for the samples annealed at the same temperature but prepared at different laboratories.

The appearance of room-temperature magnetism in TiO_2 -based materials containing cobalt only for the anatase structure is in agreement with most of the experimental results published for the Ti-O-Co system^{16–20} while scarce experiments are reported for R - TiO_2 .²¹

However, the appearance of magnetism just after a short milling is surprising as no diffusion or strong interaction is expected at this stage. Such behavior indicates some interaction between TiO_2 and Co_3O_4 just after milling. The weak ferromagnetic signal suggests that only a small part of the material exhibits ferromagnetic behavior, which is consistent with the nonferromagnetic behavior of TiO_2 and Co_3O_4 , the only phases observed by XRD in the ferromagnetic samples. The magnetic signal could then arise at the interfaces between both oxides, which are modified in the first stages of the reaction and are not detected by XRD since they represent a very small fraction of the whole material.

In order to confirm that this early interaction leads to a modification of the electronic configuration of the oxides, we performed optical measurements. Optical reflection spectra for the samples with 5% Co_3O_4 after the different thermal treatments are presented in Fig. 5. Results for the samples containing 1% Co_3O_4 were similar (although the features arising from the Co_3O_4 are not so clearly resolved).

Both A- TiO_2 and R - TiO_2 samples exhibit slight shifts in the edge after milling. This process acts as a very efficiency

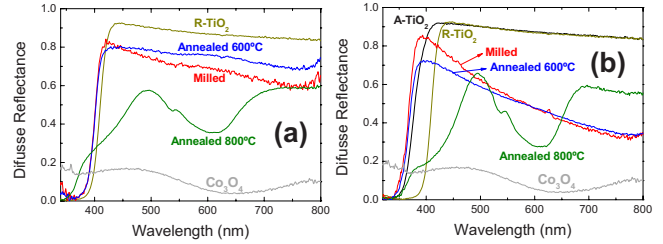


FIG. 5. (Color online) Diffuse reflectance spectra for the samples containing 5% Co_3O_4 prepared with (a) rutile and (b) anatase TiO_2 . Spectra from R - TiO_2 , A- TiO_2 , and Co_3O_4 are also presented for comparison purposes.

homogenizer procedure that favors the appearance of Co_3O_4 - TiO_2 particles contacts during the drying step because of van der Waals forces (Fig. 1). It is well known that the optical processes are very sensitive to surface effects, which may modify electronic levels or introduce new ones that can account for the observed shifts.

The samples with ferromagnetic behavior (those prepared with anatase and mixed and low-temperature annealed) exhibit a maximum in the reflectance at the edge (390–400 nm) which is absent in all the other samples. This maximum is the combination of the TiO_2 edge and a broad absorption band in the green-red part of the spectrum. Actually, the magnetic samples are the only ones exhibiting a blue coloration.²² It is particularly noteworthy that the equivalent samples prepared with R - TiO_2 show gray color.

Blue color is characteristic of compounds containing Co^{+2} atoms in octahedral positions.²³ However, Co_3O_4 has spinel structure with the Co^{+2} ions in tetrahedral (T) positions and the Co^{+3} ions in octahedral (O) ones.¹⁴ Thus, the blue color could be explained by a reduction of the Co^{+3} ions in O positions to Co^{+2} due to the interaction with the A- TiO_2 . In order to check this hypothesis, we performed x-ray absorption spectroscopy in the Co K edge.

Figure 6 presents the XAS spectra at the Co K edge of pure Co_3O_4 and samples 95% TiO_2 -5% Co_3O_4 samples prepared with A- TiO_2 and R - TiO_2 .

The spectra [Fig. 6(a)] are very similar as expected since interaction between both oxides is limited to a narrow sur-

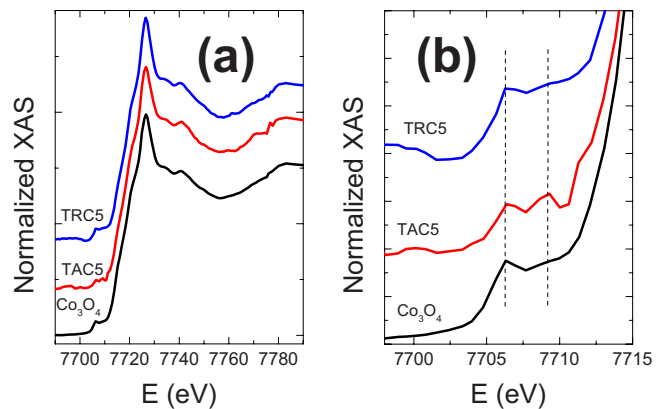


FIG. 6. (Color online) (a) XANES spectra at the Co K edge for pure Co_3O_4 and samples 95% TiO_2 -5% Co_3O_4 samples prepared with A- TiO_2 (TAC5) and R - TiO_2 (TRC5). (b) Detail of the pre-edge region.

face region. No clear shift of the edge is found. However, the detail of the prepeak shown in Fig. 6(b) evidences some changes. The feature in the Co_3O_4 spectra at about 7707 eV corresponds to a bound $1s$ - $3d$ transition of tetrahedrally coordinated metal ions^{24,25} which is forbidden for positions with a center of inversion as octahedral ones. Therefore, for Co_3O_4 , this peak is characteristic of Co^{+2} in tetrahedral positions. The prepeak feature is very similar for the sample prepared with R - TiO_2 confirming the weak interaction between TiO_2 and Co_3O_4 after milling in this sample. On the contrary, for the sample with A - TiO_2 , the peak is reduced and splits into two, corroborating the modification of the Co electronic structure. The appearance of a peak at about 7709 eV has been ascribed to Co in octahedral position with a lower oxidation state,²⁶ which agrees with results of the optical spectroscopy and confirms the surface $\text{Co}^{+3} \rightarrow \text{Co}^{+2}$ reduction in these sample. In our case, the vicinity of Ti atoms may break the octahedral symmetry inducing a distortion that can allow the presence of the prepeak. Calculations (not presented here) of the x-ray appearance near-edge structure (XANES) spectrum for a $\text{TiO}_2/\text{Co}_3\text{O}_4$ interface with Co^{+2} in octahedral positions showed a double prepeak at the same positions than those observed experimentally. A similar behavior was observed for the samples annealed at 500 and 600 °C that exhibit also ferromagnetic signals.²² These results confirm that the early interaction of the Co_3O_4 with the A - TiO_2 induces the reduction of the Co^{+3} in O positions to Co^{+2} , while this effect is not observed in the samples prepared with R - TiO_2 . Concerning the origin of the interaction, an electrochemical solid state reaction taking place at the oxides surface has been proposed.²⁷

Optical and XAS spectroscopy studies point on the Co reduction as the origin of the ferromagnetic signal. As indicated above, Co_3O_4 presents the spinel structure as most of the ferrimagnetic materials, such as Fe_3O_4 or NiCo_2O_4 , with the Co^{+2} ions in T positions and the Co^{+3} ions in O ones.¹⁴ For this structure, the predominant interaction is the antiferromagnetic superexchange between T and O positions, while interactions T - T and O - O are also antiferromagnetic but much weaker than the T - O one. Consequently, there are two magnetic sublattices corresponding to T and O positions with antiparallel orientation. Therefore, these ferrite-type spinels exhibit ferrimagnetic behavior with high order temperature ($T_C=858$ K for Fe_3O_4 , or 673 K for NiCo_2O_4). However, for Co_3O_4 , Co^{+3} ions in O positions present no magnetic moment due to the large splitting of the $3d$ orbital in this symmetry.¹⁴ Hence, in Co_3O_4 only Co^{+2} in T position holds a magnetic moment and the T - T weak antiferromagnetic interaction is the dominant one, so the system present antiferromagnetic behavior with a much lower order temperature of $T_N=42$ K. However, for Co^{+2} atoms in an octahedral field, the orbital splitting is quite small and a Co^{+2} atom in this symmetry should hold a magnetic moment.¹⁴ For a region of the crystal where Co^{+3} in O positions are reduced to Co^{+2} there should be magnetic moments in both O and T positions

with partially filled t_{2g} orbitals. In this situation, the T - O antiferromagnetic interaction would be the dominant one and the system should present a behavior similar to that of Fe_3O_4 , that is, ferrimagnetism with high order temperature (due to the strong interaction T - O). Consequently, the observed weak ferromagnetic signal can be explained by the reduction of Co^{+3} in O positions to Co^{+2} demonstrated by XANES and optical spectra, and no new magnetic ordering mechanisms are required to account for it. However, the effect in Co_3O_4 will be restricted to very small surface regions; the spinel structure of Co_3O_4 is unstable if a large fraction of Co^{+3} is reduced to Co^{+2} promoting the transformation to CoO which is antiferromagnetic. Thus, it is not possible to obtain a bulk ferrimagnetic material nor a material with uniform magnetic properties based on this effect.

Surface is the most sensitive part of the materials to any kind of treatment or interaction. Thus, nominally identical oxides from different suppliers can present identical bulk properties but fairly different surfaces. Properties depending on the surface and its reactivity in the first stages can be completely different, as we found for the three sets of samples analyzed here. This experimental fact could account for the discrepancies in results from different groups that use powder nominally identical with the same bulk structure but different surfaces due to different origin. This idea is also supported by recent results²⁸ that show that a precalcination (just at 400 °C) of ZnO alters its surface electronic structure and consequently its reactivity.

IV. CONCLUSIONS

In summary, we have demonstrated that a weak interaction between Anatase- TiO_2 and Co_3O_4 surface induces a surface reduction of Co^{+3} atoms in octahedral positions to Co^{+2} generating a weak ferromagnetic signal at room temperature. This magnetic signal can be explained as due to superexchange interactions (as the situation is similar to that in Fe_3O_4) and no new magnetic ordering mechanisms are required to account for it. This demonstrates the possibility of observing weak ferromagnetic signals in samples containing Ti, O, and Co that must be considered when studying the magnetic properties of $\text{Co}:\text{TiO}_2$ diluted magnetic semiconductors and similar materials.

ACKNOWLEDGMENTS

This work was supported by the Spanish Council for Scientific Research through the CSIC Projects No. 2006-50F0122 and No. 2007-50I015 and Spanish Ministry of Science and Education through the Projects No. MAT2007-66845-C02-01 and No. FIS-2008-06249. We acknowledge the European Synchrotron Radiation Facility for provision of synchrotron radiation facilities, and we would like to thank the SpLine CRG Beamline staff for assistance during x-ray absorption experiments.

*Corresponding author; ma.garcia@fis.ucm.es

- ¹K. Ando, *Science* **312**, 1883 (2006); H. Ohno, *ibid.* **281**, 951 (1998).
- ²K. R. Kittilstved, N. S. Norberg, and D. R. Gamelin, *Phys. Rev. Lett.* **94**, 147209 (2005).
- ³J. M. D. Coey, M. Venkatesan, and C. B. Fitzgerald, *Nature Mater.* **4**, 173 (2005).
- ⁴K. R. Kittilstved and D. R. Gamelin, *J. Am. Chem. Soc.* **127**, 5292 (2005).
- ⁵K. R. Kittilstved, W. K. Liu, and D. R. Gamelin, *Nature Mater.* **5**, 291 (2006).
- ⁶A. Brinkman, M. Huijben, M. van Zalk, J. Huijben, U. Zeitler, J. C. Maan, W. G. van der Wiel, G. Rijnders, D. H. A. Blank, and H. Hilgenkamp, *Nature Mater.* **6**, 493 (2007).
- ⁷M. S. Martín-González, J. F. Fernández, F. Rubio-Marcos, I. Lorite, J. L. Costa-Krämer, A. Quesada, M. A. Bañares, and J. L. G. Fierro, *J. Appl. Phys.* **103**, 083905 (2008).
- ⁸J. M. D. Coey and S. A. Chambers, *MRS Bull.* **33**, 1053 (2008).
- ⁹J. L. Costa-Krämer, F. Briones, J. F. Fernandez, A. C. Caballero, M. Villegas, M. Diaz, M. A. García, and A. Hernando, *Nanotechnology* **16**, 214 (2005).
- ¹⁰M. A. Garcia, M. L. Ruiz-Gonzalez, A. Quesada, J. L. Costa-Kramer, J. F. Fernandez, S. J. Khatib, A. Wennberg, A. C. Caballero, M. S. Martin-Gonzalez, M. Villegas, F. Briones, J. M. Gonzalez-Calbet, and A. Hernando, *Phys. Rev. Lett.* **94**, 217206 (2005).
- ¹¹A. Quesada, M. A. García, M. Andrés, A. Hernando, J. F. Fernández, A. C. Caballero, M. S. Martín-González, and F. Briones, *J. Appl. Phys.* **100**, 113909 (2006).
- ¹²M. A. Garcia, E. Fernandez Pinel, J. de la Venta, A. Quesada, V. Bouzas, J. F. Fernández, J. J. Romero, M. S. Martín González, and J. L. Costa-Krämer, *J. Appl. Phys.* **105**, 013925 (2009).
- ¹³J. S. Stickler, S. Kern, A. Wold, and G. S. Heller, *Phys. Rev.* **164**, 765 (1967).
- ¹⁴W. L. Roth, *J. Phys. Chem. Solids* **25**, 1 (1964).
- ¹⁵S. R. Yoganarasimhan and C. N. R. Rao, *Trans. Faraday Soc.* **58**, 1579 (1962).
- ¹⁶Y. Matsumoto, M. Murakami, T. Shono, T. Hasegawa, T. Fukumura, M. Kawasaki, P. Ahmet, T. Chikyow, S. Koshihara, and H. Koinuma, *Science* **291**, 854 (2001).
- ¹⁷S. R. Shinde, S. B. Ogale, S. Das Sarma, J. R. Simpson, H. D. Drew, S. E. Lofland, C. Lanci, J. P. Buban, N. D. Browning, V. N. Kulkarni, J. Higgins, R. P. Sharma, R. L. Greene, and T. Venkatesan, *Phys. Rev. B* **67**, 115211 (2003).
- ¹⁸J. S. Higgins, S. R. Shinde, S. B. Ogale, T. Venkatesan, and R. L. Greene, *Phys. Rev. B* **69**, 073201 (2004).
- ¹⁹K. A. Griffin, A. B. Pakhomov, C. M. Wang, S. M. Heald, and K. M. Krishnan, *Phys. Rev. Lett.* **94**, 157204 (2005).
- ²⁰H. Toyosaki, T. Fukumura, Y. Yamada, K. Nakajima, T. Chikyow, T. Hasegawa, H. Koinuma and M. Kawasaki, *Nature Mater.* **3**, 221 (2004).
- ²¹Y. Matsumoto, R. Takahashi, M. Murakami, T. Koida, X. Fan, T. Hasegawa, T. Fukumura, M. Kawasaki, S. Koshihara, and H. Koinuma, *Jpn. J. Appl. Phys., Part 2* **40**, L1204 (2001).
- ²²See EPAPS Document No. E-PRBMDO-79-085910 for a photograph showing the samples coloration and the XANES spectra of the samples annealed at 500 and 600 °C. For more information on EPAPS, see <http://www.aip.org/pubservs/epaps.html>.
- ²³D. Sutton, *Electronic Spectra of Transition Metal Complexes* (McGraw-Hill, Berkshire, England, 1975).
- ²⁴M. F. F. F. Lelis, A. O. Porto, C. M. Gonçalves, and J. D. Fabris, *J. Magn. Magn. Mater.* **278**, 263 (2004).
- ²⁵T. Jiang and D. E. Ellis, *J. Mater. Res.* **11**, 2242 (1996).
- ²⁶J. Jason, A. E. C. Palmqvist, E. Fridell, M. Skoglundh, L. Österlund, P. Thormählen, and V. Langer, *J. Catal.* **211**, 387 (2002).
- ²⁷M. S. Martín-González (private communication).
- ²⁸F. Rubio-Marcos, A. Quesada, M. A. García, M. A. Bañares, J. L. G. Fierro, M. S. Martín-Gonzalez, J. L. Costa-Krämer, and J. F. Fernández, *J. Solid State Chem.* (to be published).